Proceedings of the 2009 IEEE International Conference on Networking, Sensing and Control, Okayama, Japan, March 26-29, 2009

Application of DT Method to Bifurcation Analysis of Microcandilevers with Proportional-Plus-Derivative Control

C. C. Wang, H. T. Yau, M. J. Jang, Y. L. Yeh, and T. T. Liao

Abstract—**This paper studies the bifurcation behavior of the probe tip of an atomic force microscope with a proportional-plus-derivative (PD) feedback control using the DT (differential transformation) method. The dynamic behavior of the probe tip with PD control law is characterized by reference to maximum Lyapunov exponent plots produced using the time-series data obtained from differential transformation method. Furthermore, the detailed transitions in the dynamic response of the probe tip are examined using bifurcation diagrams of the tip displacement and the tip velocity, respectively. The results indicate that the probe tip behavior is significantly dependent on the magnitude of the proportional and derivative control gain. Specifically, the probe tip motion includes T-, 2T-, 3T-, 4T-, multi-periodic, and chaotic motion. Numerical results show that the dynamic behavior will leave chaotic motion to periodic motion at *Kp*=-0.45 in the steady state by changing the control loop gain *Kv* from -0.1 to -1.0. Furthermore, it is demonstrated that the differential transformation method is in good agreement for the considered system.**

I. Introduction

THE atomic force microscope (AFM) provides a powerful tool for surface analysis applications in the nano-electronics, materials and biotechnology fields. During operation, intermolecular forces between the AFM probe tip and the sample surface cause a deflection of the microcantilever on which the probe tip is mounted. The variation in force acting on the tip is then evaluated by using some form of optical technique to measure the deflection of the cantilever.

The nonlinear dynamic behavior of an AFM system is a major concern since any irregular motion of the AFM probe tip inevitably degrades the precision of the measurement results. Burnham et al. [1], [2] showed that the microcantilever of an AFM performed chaotic motion under specific physical conditions. Ashhab et al. [3] modeled the microcantilever of an AFM using a single-frequency mode approximation and analyzed the chaotic dynamics of the cantilever-sample system using the Melnikov method. Lee et al. [4] analyzed the effects of van der Waals and Derjaguin-Muller-Toporov forces on the tip-sample interactions induced in dynamic force microscopy (DFM). The authors also presented detailed experimental results which provided valuable new perspectives and insights into DFM. Ruetzel et al. [5] applied the Galerkin method to investigate the nonlinear dynamics of an AFM probe tip under the assumption that the tip-surface interactions were governed by Lennard-Jones potentials. Based upon their analysis, the authors showed that the probe tip exhibited a broad range of dynamic phenomena, including both periodic and chaotic motion.

However, none of the studies reviewed above presented phase portraits, power spectra, Poincaré maps, maximum Lyapunov exponent plots or bifurcation diagrams to confirm the validity of their predictions for the AFM behavior or use a PD (proportional-plus-derivative) feedback to control the chaotic motion observed in the AFM system. Accordingly, the present study investigates the dynamic behavior of an AFM probe tip using two numerical methods, namely the differential transformation method [6], [7] and the Runge-Kutta method and then characterizes the dynamic response of the system by reference to phase portraits, power spectra, Poincaré maps, and maximum Lyapunov exponent plots. Finally, the chaotic behavior in the AFM system is identified using bifurcation diagrams of the tip displacement and tip velocity, respectively and a PD controller included proportional gain and derivative gain is applied to control this system.

The remainder of this paper is organized as follows. Section 2 presents a mathematical model for the time-dependent motions of the microcantilever tip and describes the solution of this model using the differential transformation method. Section 3 compares and contrasts the numerical results obtained by the differential transformation method and the Runge-Kutta method for the dynamic response of the microcantilever tip at various proportional gains and derivative gains. Subsequently, the nonlinear dynamic behavior of the probe tip is analyzed by maximum Lyapunov exponent plots and bifurcation diagrams, respectively. Finally, Section 4 draws some brief conclusions.

Manuscript received October 1, 2008. This work was supported by National Science Council of the R.O.C. under Grant No. NSC-97-2221-E-269-022, NSC-97-2221-E-269-009, 97-2221-E-269-012, and 97-2221-E-269-008.

C. C. Wang is with the Far East University, No. 49 Chung-Hua Road, Hsin-Shih, Tainan, Taiwan(corresponding author to provide phone: 886-6-597-9566; fax: 886-6-597-7115; e-mail: ccwang@cc.feu.edu.tw).

H. T. Yau is with the Electrical Engineering Department, Far East Univ. No. 49 Chung-Hua Road, Hsin-Shih, Tainan, Taiwan(e-mail: htyau@cc.feu.edu.tw).

M. J. Jang is with the vice president of Far East Univ., (e-mail: mjjang@cc.feu.edu.tw).

Y. L. Yeh is with the Automation and Control Department, Far East University, No. 49 Chung-Hua Road, Hsin-Shih, Tainan, Taiwan(e-mail: yehyl@cc.feu.edu.tw).

T. T. Liao is with the Mechanical Engineering Dept., Far East Univ., No. 49 Chung-Hua Road, Hsin-Shih, Tainan, Taiwan(e-mail: liao_ssg@seed.net.tw).

II. MATHEMATICAL MODELING

The behavior of an AFM probe tip in which the tip-surface interactions are governed by the Lennard-Jones potential function can be modeled using the following non-dimensional single-degree-of-freedom model: [5]

$$\dot{X}_1 = X_2 \tag{1}$$

$$\dot{X}_2 = -X_1 + \frac{A_1}{(Z-X_1)^2} - \frac{A_1 A_2{}^6}{30(Z-X_1)^8} + A_3 \sin\Omega\tau + A_3 A_4 \Omega \cos\Omega\tau - A_4 X_2 \tag{2}$$

In the above, X_1 indicates the non-dimensionalized displacement of the microcantilever tip (where a positive value indicates a displacement towards the sample), X_2 denotes the non-dimensionalized microcantilever tip velocity of the microcantilever, and Z is the vibrational amplitude of the dither piezoelectric actuator which drives the tip. Note that both X_1 and Z are non-dimensionalized by the gap between the tip and the sample under equilibrium conditions. In the case where the excitation frequency is close to the natural frequency of the microcantilever, Ω=1. Furthermore, assuming a Si–Si probe-sample system, the coefficients in (2) have the following values: A_1 = 4/27, A_2 =0.3, A_3 = 0.5, and A_4= 0.03.

In most AFM systems, the state X_1 is measured, and the state X_2 can be estimated. This makes it possible to apply a PD (proportional-plus-derivative) control force of the form $u = X_1 K_p + X_2 K_v$ to the cantilever. In this case, the state equations of the system are written as

$$\dot{X}_1 = X_2 \tag{3}$$

$$\dot{X}_2 = -X_1 + \frac{A_1}{(Z-X_1)^2} - \frac{A_1 A_2{}^6}{30(Z-X_1)^8} + A_3 \sin\Omega\tau + A_3 A_4 \Omega\cos\Omega\tau - A_4 X_2 + KpX_1 + KvX_2 \tag{4}$$

We can see that applying the above state feedback control is equivalent to change stiffness and damping in the system independently. If K_p > 1 or K_v > A_4, the stiffness or damping is negative and causes the system unstable and even diverge. Therefore, we will restrict our analysis to the case when K_p < 1 and K_v < A_4.

Differential transformation is one of the most widely used of all techniques for solving differential equations due to its rapid rate of convergence and its minimal computational error. Furthermore, compared to the integral transformation approach, differential transformation has the further advantage that it can be used to solve nonlinear differential equations. In solving (3) and (4) using the differential transformation method, the AFM system model is transformed with respect to the time domain τ, and hence the two equations become

$$\frac{k+1}{H}\bar{X}_1(k+1) = \bar{X}_2(k) \tag{5}$$

$$\frac{k+1}{H}\bar{X}_2(k+1) = -\bar{X}_1(k) + \frac{A_1}{(1-\bar{X}_1(k))^2} - \frac{A_1 A_2{}^6}{(1-\bar{X}_1(k))^8} + A_3 \cdot \frac{(\Omega H)^k}{k!}\sin\left(\frac{\pi k}{2}\right) + A_3 A_4 \Omega \frac{(\Omega H)^k}{k!}\cos\left(\frac{\pi k}{2}\right) - A_4 \bar{X}_2(k) + Kp\bar{X}_1(k) + Kv\bar{X}_2(k) \tag{6}$$

III. RESULTS AND DISCUSSIONS

A. Numerical Simulation Results

As discussed above, the nonlinear behavior of the AFM tip displacement is analyzed in this study using the differential transformation method (DTM). The dynamic behavior of the AFM system is characterized by reference to power spectra, Poincaré maps, maximum Lyapunov exponent plots and bifurcation diagrams produced using the time-series data for the displacement and velocity of the microcantilever tip. Note that in producing these various plots, the time-series data corresponding to the first 1000 revolutions are deliberately excluded in order to ensure that the results reflect steady-state conditions.

Table 1 compares the results obtained by the DTM and the Runge-Kutta method (RKM) for the displacement and velocity of the microcantilever tip at various values of K_p. It is seen that a good agreement exists between the two sets of numerical results. Table 2 clarifies the effect of the time-step value on the Poincaré maps for the microcantilever tip at different values of K_v. It can be seen that for a given K_v, the tip displacement and velocity values calculated using different values of the time step are in agreement to approximately 4~5 decimal places.

TABLE I
COMPARISON OF POINCARÉ MAPS OF TIP DISPLACEMENT AND VELOCITY CALCULATED USING DTM AND RKM METHODS, RESPECTIVELY. (K_v = 0)

method	K_p	X_1 (n T)		X_2 (n T)	
		H=10^{-3}	H =10^{-2}	H =10^{-3}	H =10^{-2}
DTM	-0.5	0.05602	0.05601	1.18592	1.18593
RKM		0.05604	0.05602	1.18595	1.18592
DTM	-1.0	0.05224	0.05224	1.17584	1.17585
RKM		0.05224	0.05224	1.17581	1.17585

TABLE II
COMPARISON OF POINCARÉ MAPS OF TIP DISPLACEMENT AND VELOCITY AT DIFFERENT VALUES OF TIME STEP, H. (K_p = 0)

K_v = -1.06		
H	X_1 (n T)	X_2 (n T)
π/200	-1.2428790523	0.2502006706
π/400	-1.2428191181	0.2502433259
K_v = 0.02		
H	X_1 (n T)	X_2 (n T)
π/200	-1.8156736640	1.4155961246
π/400	-1.8156916564	1.4155523452

B. Situation 1

In the first situation, the bifurcation parameter was chosen to be the K_p, and K_v=0. In the current study, Figs. 1 plot the bifurcation diagrams of the tip displacement and the tip velocity, respectively, taking K_p as the bifurcation parameter. Finally, Figs. 2(a)-2(f) present the maximum Lyapunov exponent of the microcantilever tip trajectory at K_p = -0.5, -0.47, -0.39, -0.32, -0.22, -0.21, -0.08 and -0.05, respectively.

Figs 1(a)(b) and 2(a) show that at lower values of K_p, i.e. K_p <-0.47, the displacement (X_1) and velocity (X_2) of the tip both exhibit a dynamic periodic response. As K_p is increased from -0.47 to -0.41, Figs. 1(a) and 1(b) show that both the tip displacement and the tip velocity perform chaotic motions. Fig. 2(b) presents the maximum Lyapunov exponent at K_p = -0.47 and proof the appearance of chaos. At K_p = -0.4, the chaotic motion is replaced by multi-subharmonic motion, as shown in Figs. 1(a) and 1(b). When K_p is increased over the interval -0.4≤K_p<-0.32, the tip response includes both multi-subharmonic and 4T-subharmonic motion. Fig. 2(c) presents the maximum Lyapunov exponent at K_p =-0.39(4T). However, at K_p =-0.32, the 4T-periodic motion is replaced by chaotic motion, as shown in Fig. 2(d). Thereafter, the chaotic motion changes its unstable state at K_p =-0.22 and is replaced by multi-subharmonic motion. In the range -0.22≤ K_p <0.1, Figs. 1(a) and 1(b) show that both the tip displacement and the tip velocity perform 4 kinds of motions including T-, 3T-, 4T-, and multi-subharmonic motions. Figs. 2(e)-2(h) present the maximum Lyapunov exponent corresponding to K_p = -0.22, -0.21, -0.08 and -0.05, and the maps confirm the existence of multi-, 4T-, 3T-subharmonic and T-periodic behavior shown in the bifurcation diagrams.

From the discussions above, it is clear that the dynamic response of the probe tip depends on the magnitude of K_p. The various motions performed by the tip as K_p increases from -2 to 0.1 are summarized in Table 3.

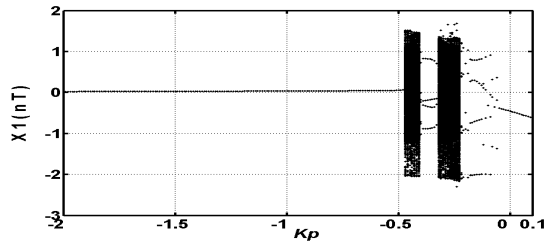

(a)

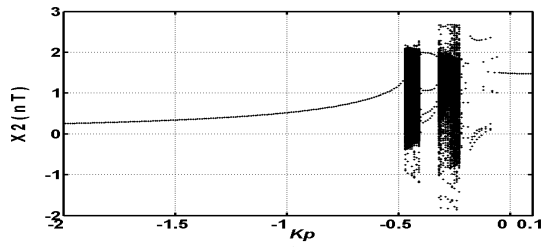

(b)

Fig. 1. Bifurcation diagrams for (a) tip displacement and (b) tip velocity using K_p as the bifurcation parameter.

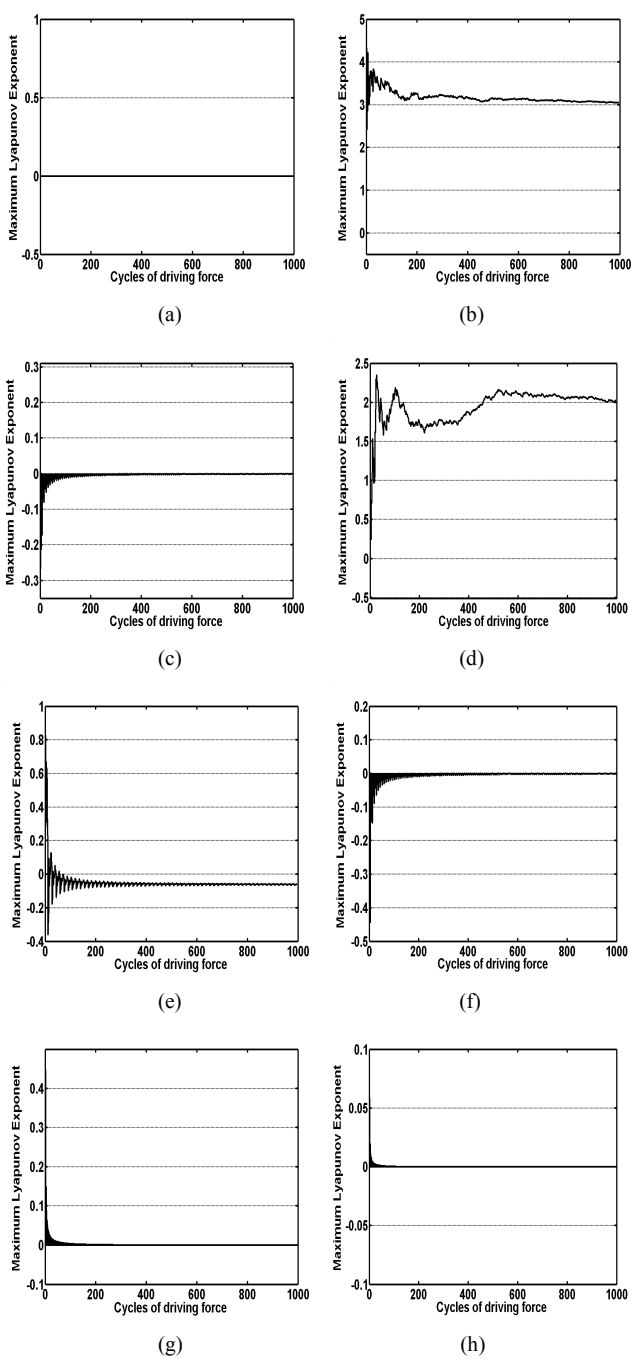

(a) (b) (c) (d) (e) (f) (g) (h)

Fig. 2. Maximum Lyapunov exponents of microcantilever tip at different values of K_p: (a) -0.5, (b) -0.47, (c) -0.39, (d) -0.32, (e) -0.22, (f) -0.21, (g) -0.08, and (h) -0.05.

TABLE III
VARIATION OF MICROCANTILEVER TIP RESPONSE WITH KP OVER INTERVAL $-2< K_P <0.1$.

K_p	(-2, -0.47)	[-0.47,-0.4)	[-0.4,-0.39)	[-0.39,-0.32)
Dynamic Behavior	T	chaos	multi-period	4T
K_p	[-0.32,-0.22)	[-0.22,-0.21)	[-0.21,-0.1)	[-0.1,-0.09)
Dynamic Behavior	chaos	multi-period	4T	T
Kp	[-0.09,-0.08)	[-0.08,-0.05)	[-0.05,0.1)	
Dynamic Behavior	4T	3T,T	T	

C. Situation 2

In the second situation, the bifurcation parameter was chosen to be the K_v, and K_p =0.

Figs. 3(a) and 3(b) plot the bifurcation diagrams of the tip displacement and the tip velocity, respectively, taking K_v as the bifurcation parameter. It is shown that at lower values of K_v, i.e. K_v <-1.03, the displacement (X_1) and velocity (X_2) of the tip both exhibit a dynamic periodic response. As the value of K_v is increased from -1.03 to -1.01, the T-periodic motion is replaced by 2T- and 4T-subharmonic motions. Figs. 4(a), 4(b) and 4(c) present the maximum Lyapunov exponent at K_v =-1.06(T), -1.03(2T) and -1.01(4T), respectively. The subharmonic motion changes its stability at K_v =-1.0 and is replaced by chaotic motion, as shown in Figs. 3(a)(b) and 4(d). When *Kv* is increased over the interval $-1.0\leq K_v <-0.98$, the tip performs chaotic motion. However, as K_v is further increased over the interval $-0.98\leq K_v <0.1$, the chaotic response is disappeared and the tip exhibits T-periodic motion. Figs. 4(e) and 4(f) present the maximum Lyapunov exponent corresponding to K_v =-0.98 and 0.02, and the exponents are both less than 1 to guarantee the appearance of T-periodic motion.

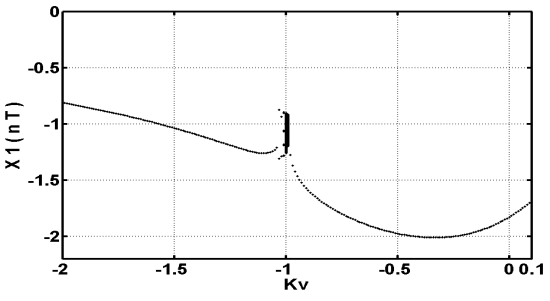

(a)

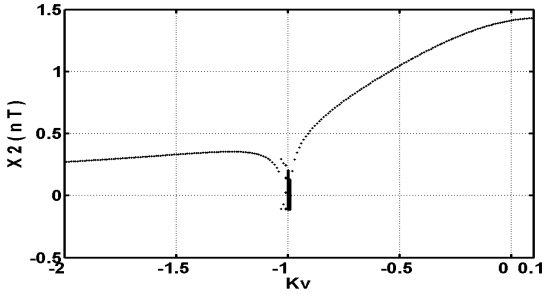

(b)

Fig. 3. Bifurcation diagrams for (a) tip displacement and (b) tip velocity using K_v as the bifurcation parameter.

From the discussions above, the various motions performed by the tip as K_v increases from -2.0 to 0.1 are summarized in Table 4. In general, the results show that depending on the value of K_v, the tip may exhibit periodic behavior, i.e. T-, 2T- or 4T- subharmonic motion, or a chaotic response.

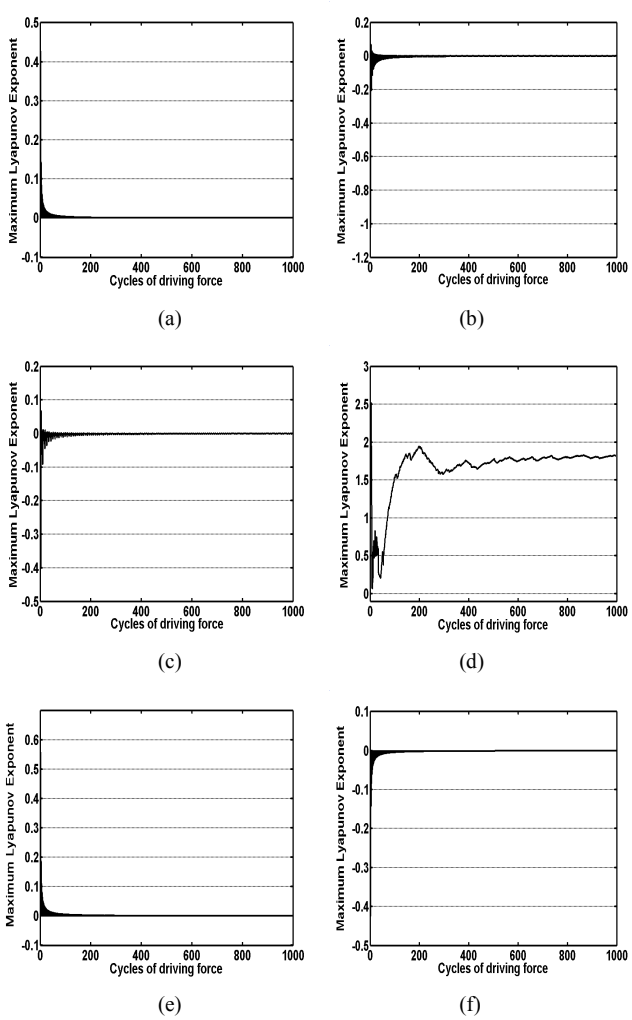

(a) (b) (c) (d) (e) (f)

Fig. 4. Maximum Lyapunov exponents of microcantilever tip at different values of K_v: (a) -1.06, (b) -1.03, (c) -1.01, (d) -1.0, (e) -0.98, and (f) 0.02.

TABLE Ⅳ
VARIATION OF MICROCANTILEVER TIP RESPONSE WITH KV OVER INTERVAL $-2< K_v <0.1$.

K_v	(-2, -1.03)	[-1.03,-1.01)	[-1.01,-1.0)	[-1.0,-0.98)	[-0.98,0.1)
Dynamic Behavior	T	2T	4T	chaos	T

D. Situation 3

In order to analyze that the influence of both K_p and K_v, the case is restricted $K_p < 1$ and $K_v < A_4$. Also, the PD feedback is used to control this system to avoid the chaotic motion appear. The bifurcation parameter was chosen to be the K_v at K_p =-0.45.

Figs. 5(a)(b) and 6(a) show that at lower values of K_v, i.e. K_v <-0.1, the displacement (X_1) and velocity (X_2) of the tip both exhibit a dynamic periodic response. At K_v = -0.1, the T-periodic motion is replaced by chaotic motion, as shown in Figs. 5 and 6(b). When K_v is increased over the interval -0.1≤ K_v <0.13, the tip response is chaotic motion. Figs. 6(c) and 6(d) present the maximum Lyapunov exponent at K_v = 0 and 0.02, respectively.

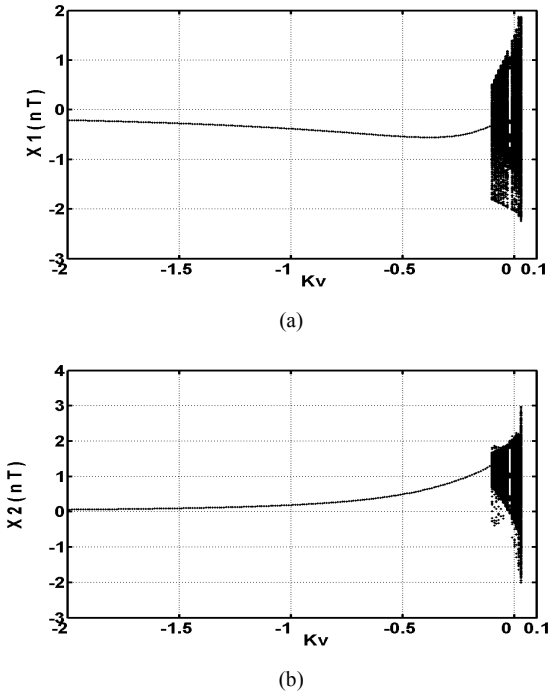

Fig. 5. Bifurcation diagrams for (a) tip displacement and (b) tip velocity using K_v as the bifurcation parameter.

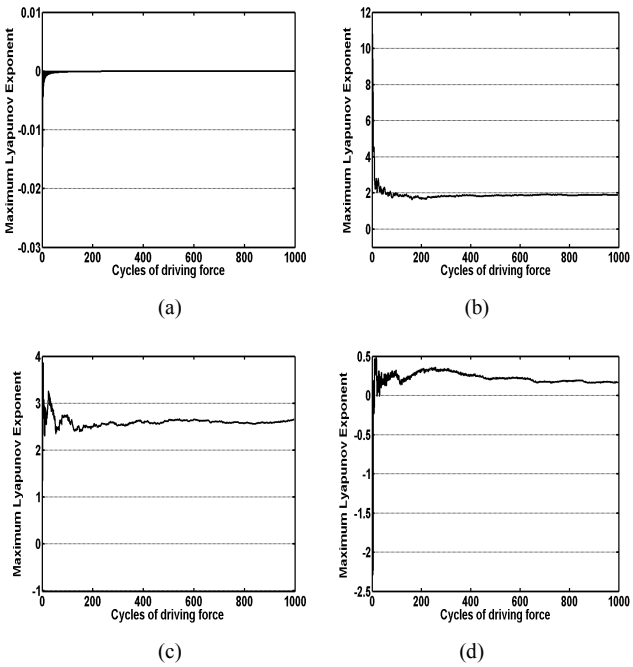

Fig. 6. Maximum Lyapunov exponents of microcantilever tip at different values of K_v : (a)-1.0, (b)-0.1, (c)0, and (d)0.02.

It is known that if the tip of the AFM system operates in the state of aperiodic motion, the resulting broadband vibration with large amplitude will lead to a higher probability of fatigue failure of microcantilever and decrease the measure accuracy of the AFM system. At K_p =-0.45 and K_v =-0.1, the maximum Lyapunov exponent is positive and Poincaré map demonstrated a fractal structure. It shows that the trajectory of the tip displacement is in a state of chaos. In order to eliminate the system operating in a no synchronous motion, a decreased derivative gain K_v =-0.1 is applied to control this system. From Fig. 7, it can be seen that the tip dynamics leave the disorder state and turns to a periodic motion in the steady state after the derivative gain changes from -0.1 to -1.0.

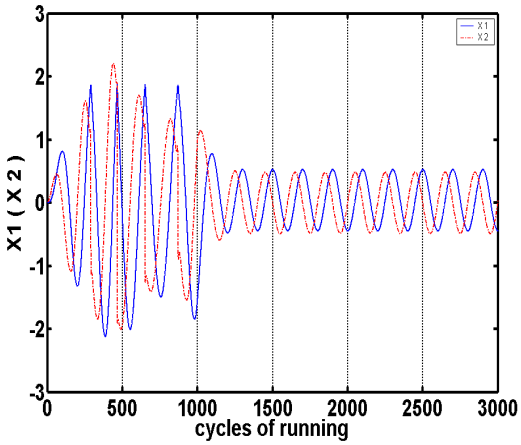

Fig. 7. The time responses of tip dynamics at K_v =-0.1with K_v =-0.1 changes to K_v =-1.0 from 1000 cycles running.

IV. Conclusion

This study has applied the differential transformation method to investigate the dynamic behavior of an AFM probe tip with PD feedback control. Phase trajectories, Poincaré maps, maximum Lyapunov exponent plots, and bifurcation diagrams have been used to characterize the dynamic response of the AFM tip probe as a function of the proportional and derivative gains and to detect the onset of chaotic motion. In general, the results have shown that as the proportional gain is increased from -0.47 to -0.22, the probe tip motion changes initially from T-periodic to chaotic motion, and then from chaotic to multi-periodic, and finally to chaotic motion. And, when the derivative gain is increased from -1.01 to 0.1, the probe tip motion changes initially from 4T-periodic to chaotic motion, and finally to T-periodic motion. In order to eliminate the system operating in a no synchronous motion, a decreased derivative gain is applied to control this system. It is obtained that the tip dynamics leave the disorder state and turns to a periodic motion in the steady state after the derivative gain changes from -0.1 to -1.0.

Acknowledgment

The financial support provided to this research by the National Science Council of the R.O.C. under Grant No. NSC-97-2221-E-269-022, NSC-97-2221-E-269-009, 97-2221-E-269-012, and 97-2221-E-269-008 are greatly appreciated.

References

[1] N. A. Burnham, R. J. Colton, and H. M. Pollock, "Interpretation of force curves in force microscopy," *Nanotechnology*, vol. 4, pp. 64-80, 1993.

[2] N. A. Burnham, A. J. Kulik, G. Germaud, and G. A. D. Briggs, "Nanosubharmonics: the dynamics of small nonlinear contacts," *Phys. Rev. Lett.*, vol. 74, pp. 5092-5095, 1995.

[3] M. Ashhab, M. V. Salapaka, M. Dahleh, and I. Mezic, "Melnikov-based dynamical analysis of microcantilevers in scanning probe microscopy," *Nonlinear Dyn*, vol. 20, pp. 197–220, 1999.

[4] S. I. Lee, S. W. Howell, A. Raman, and R. Reifenberger, "Nonlinear dynamic perspectives on dynamic force microscopy," *Ultramicroscopy*, vol. 97, pp. 185–198, 2003.

[5] S. Ruetzel, S. I. Lee, and A. Raman, "Nonlinear dynamics of atomic-force-microscope probes driven in Lennard-Jones potentials," *Proc. R. Soc. London A*, vol. 459, pp. 1925–1948, 2003.

[6] C. L. Chen, S. H. Lin, and C. K. Chen, "Application of Taylor Transformation to Nonlinear Predictive Control Problem," *Appl. Math. Modeling*, vol. 20, pp. 609-710, 1996.

[7] M. J. Jang, C. L. Chen, and Y. C. Liu, "Two-dimensional differential transform for partial differential equations," *Applied Mathematics and Computation*, vol. 121, pp. 261–270, 2001.